Generation of Linearly Chirped Microwave Waveform With an Increased Time-Bandwidth Product Based on a Tunable Optoelectronic Oscillator and a Recirculating Phase Modulation Loop

Wangzhe Li, *Member, IEEE*, and Jianping Yao, *Fellow, IEEE, Fellow, OSA*

***Abstract*—Photonic generation of a linearly chirped microwave waveform with an increased time-bandwidth product (TBWP) based on a frequency-tunable optoelectronic oscillator (OEO) and a recirculating phase modulation loop (RPML) is proposed and experimentally demonstrated, for the first time to the best of our knowledge. In the proposed system, a continuous-wave (CW) light wave is divided into two parts: one is sent to the tunable OEO to generate a frequency-tunable microwave signal and the other is intensity-modulated by a switching signal at an intensity modulator to form a chirp-free optical pulse, which are then sent to the RPML, in which the chirp-free pulse is phase modulated by a parabolic waveform to generate a linearly chirped optical waveform. The recirculation of the linearly chirped optical waveform inside the loop would lead to the waveform to experience multiple phase modulations, thus multiplying its chirp rate. By beating the chirped waveform and an optical sideband from the OEO at a high-speed photodetector (PD), a linearly chirped microwave waveform is obtained. The key significance of the approach is that the chirp rate is significantly increased, leading to a significantly increased TBWP. In addition, the approach allows the generation of a linearly chirped frequency-tunable microwave waveform without using a separate microwave source. The technique is experimentally verified. The generation of a linearly chirped microwave waveform with an increased TBWP by 16 times is demonstrated.**

***Index Terms*—Fiber Bragg grating, linear frequency modulation, microwave photonics, microwave signal generation, optoelectronic oscillator, phase modulation, radar pulse compression.**

I. Introduction

MICROWAVE pulse compression has been widely employed in modern radar systems, in which long microwave waveforms are transmitted, and then received and compressed at a radar receiver to increase the range resolution [1]. Particularly, in microwave pulse compression, a linearly chirped microwave waveform (LCMW) with a large time-bandwidth product (TBWP), in the order of 10^2 or 10^3, is required. In the electrical domain, such an LCMW can be generated using a voltage-controlled oscillator or a digital signal processing module. However, due to the limited speed and bandwidth of electronics, the central frequency and the bandwidth of an LCMW is limited to a few gigahertz [2], [3], which may not meet the requirement for applications in advanced radar systems, where the central frequency up to tens or even hundreds of gigahertz, and the bandwidth of a few gigahertz are often needed. In addition, an LCMW with a tunable carrier frequency, chirp rate and TBWP is also required for different practical applications. Numerous photonic techniques have been proposed and developed to generate LCMWs in the last few years [4]–[18]. The key advantages of using photonic techniques for LCMW generation are the high frequency and broad bandwidth offered by modern photonics, which are not possible using electronic devices.

In general, the photonic techniques for LCMW generation can be classified into three categories:

First, by beating two wavelengths that are complementarily phase modulated by a parabolic waveform at a photodetector (PD). Typically, the two wavelengths should be phase correlated, which can be generated by selecting two wavelengths from an externally modulated light wave [4]–[8] or from a mode-locked laser source [9], [10]. The two wavelengths are either spatially separated or orthogonally polarization multiplexed, thus complementary phase modulation can be applied separately to the two wavelengths to achieve complementary phase modulation. The major limitation of the approach is that the frequency tuning range of the microwave carrier and frequency agility are limited due to the use of fixed optical filters to select the two wavelengths. In addition, an external microwave source is required. Furthermore, the TBWP of the LCMWs is usually small, only in the order of 10 due to a small phase modulation index.

Second, based on space-to-time mapping (STM) [11] or frequency-to-time mapping (FTM) [12], [13]. Microwave waveform generation based on STM is usually implemented using a spatial light modulator (SLM). An SLM is a 2-D device, which can be used as a 2-D spatial filter. By passing a 2-D light beam through an SLM, the phase and the magnitude of the light beam can be changed, making the generation of an arbitrary waveform possible. The major limitation of the STM-based approach is that free-space optics is involved in the system, making the system bulky and complicated. Microwave waveform generation based on FTM can be implemented using pure fiber optics [12]. In an FTM-based system, an optical spectral shaper is employed to shape the spectrum of an ultra-short optical pulse, to make the

Manuscript received January 14, 2014; revised February 16, 2014; accepted February 28, 2014. Date of publication March 2, 2014; date of current version September 1, 2014. This work was supported by the Natural Sciences and Engineering Research Council of Canada (NSERC).

The authors are with the Microwave Photonics Research Laboratory, School of Electrical Engineering and Computer Science, University of Ottawa, Ottawa, ON K1 N 6N5, Canada (e-mail: jpyao@eecs.uottawa.ca).

Color versions of one or more of the figures in this paper are available online at http://ieeexplore.ieee.org.

Digital Object Identifier 10.1109/JLT.2014.2309392

spectrum have a shape that is a scaled version of the waveform to be generated. The major limitation of a purely fiber-optic FTM-based system is that the spectral response of the optical spectral shaper is usually fixed, thus making the generated waveform also fixed. To solve this problem, recently a reconfigurable spectral shaper implemented in a silicon platform that consists of eight cascaded micro-ring resonators [14] was proposed and demonstrated. Through thermal tuning, the spectral response of the spectral shaper can be changed, which leads to the change of the generated waveform. To generate a sophisticated waveform, however, a large number of micro-rings should be integrated in the chip, which would increase the footprint and the complexity of the chip.

Third, by beating two linearly chirped optical pulses with different chirp rates [15]–[17]. It is different from the approach in the first category, where two CW light waves are complementarily phase modulated by a parabolic waveform to generate two linearly chirped optical waveforms, here the two linearly chirped optical pulses are obtained by sending an ultra-short chirp-free pulse from a mode-locked laser (MLL) to two dispersive elements with different dispersion, leading to the generation of two optical pulses with different chirp rates. The dispersive element can be a single mode fiber, a dispersion compensating fiber, and a linearly chirped fiber Bragg grating. By beating the two pulses at a PD, an LCMW would be generated. This approach is capable of generating an LCMW with a TBWP more than 100 [16], but the reconfigurability of the system is also limited. For example, when the dispersion of the two dispersive elements is selected, the chirp rate of the LCMW is fixed.

In this paper, a photonic approach to achieving full reconfigurable LCMW generation with a large and tunable TBWP, controllable temporal duration, and tunable frequency is proposed and experimentally demonstrated. The system consists of two modules, a tunable OEO and a recirculating phase modulation loop (RPML). A continuous-wave (CW) light wave from a tunable laser source (TLS) is split into two parts: one is sent to a phase modulator (PM) in the tunable OEO to generate a frequency-tunable microwave signal and the other is sent to an intensity modulator (IM) to generate a chirp-free optical pulse. The chirp-free pulse is then sent to the RPML, circulating inside the loop to experience multiple phase modulations at a PM to increase the chirp rate. The chirped optical pulse, after reaching a pre-defined chirp rate, is routed out from the RPML by an optical switch. Then, by beating the chirped optical pulse from the RPML with one optical sideband from the OEO at a PD, an LCMW is obtained. The key significance of the technique is that an LCMW with a significantly increased chirp rate can be generated through multiple phase modulations, which would significantly increase the TBWP. In addition, the microwave carrier is generated by the OEO, thus no additional microwave source is needed. The microwave carrier frequency can also be tuned by tuning the wavelength of the TLS. Thus, full reconfigurable LCMW generation with a large and tunable TBWP, controllable temporal duration, and tunable frequency can be achieved. The technique is experimentally verified. The generation of an LCMW at 15 and 18 GHz with an increased TBWP by 16 times is demonstrated.

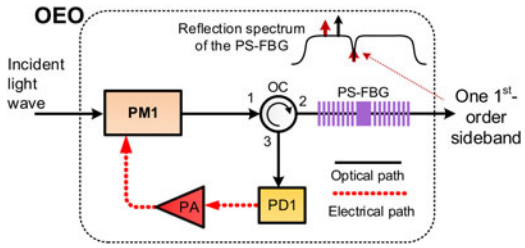

Fig. 1. Configuration of the tunable OEO.

II. Operation Principle

A. Tunable Optoelectronic Oscillator

The first module in the system is the tunable OEO. The schematic of the OEO is shown in Fig. 1. It consists of a PM (PM1), a phase-shifted fiber Bragg grating (PS-FBG) that has an ultra-narrow notch in reflection, an optical circulator (OC), a PD (PD1), and a power amplifier (PA). The joint operation of the PM and the PS-FBG corresponding a photonic microwave filter with the central frequency of the filter determined by the wavelength of the incident light wave and the wavelength of the notch [19]. When the gain provided by the PA is sufficiently high to compensate for the loss of the loop, the OEO will start to oscillate and a microwave signal with its frequency determined by the wavelength difference between the optical carrier and the notch of the PS-FBG is generated. By tuning the wavelength of the optical carrier, the frequency of the generated microwave signal is accordingly changed. Note that the ultra-narrow notch in reflection corresponds to an ultra-narrow passband in transmission. Thus, at the other end of the PS-FBG, a sideband is transmitted, as shown in Fig. 1. In the demonstration, the transmitted sideband is the lower first-order sideband. Further details about the operation of the tunable OEO can be found in [19] and [20].

B. Recirculating-Phase-Modulation Loop

The second module in the system is the RPML. The schematic of the RPML is shown in Fig. 2(a). It consists of an optical coupler, a PM (PM2), a 1×2 optical switch, and an erbium-doped fiber amplifier (EDFA). A chirp-free optical pulse generated at an IM that is controlled by a switching signal is sent to PM2 via the optical coupler. The optical pulse would be phase modulated at PM2 by a parabolic waveform to generate a chirped optical pulse. Depending on the state of the optical switch in "1"or "2", the optical pulse will be circulating in the loop or directed to the output of the loop. The switch is controlled by the same switching signal applied to the IM but with a certain delay, to make the pulse continue circulating inside the loop to reach a pre-defined chirp rate before being routed out of the loop. The parabolic waveform is generated by a microwave arbitrary waveform generator (AWG) with a time duration identical to that of the incident optical pulse. The repetition rate of the parabolic waveform is equal to the fundamental resonant frequency of the RPML so that the parabolic waveform could be synchronized with the recirculating optical pulse inside the loop.

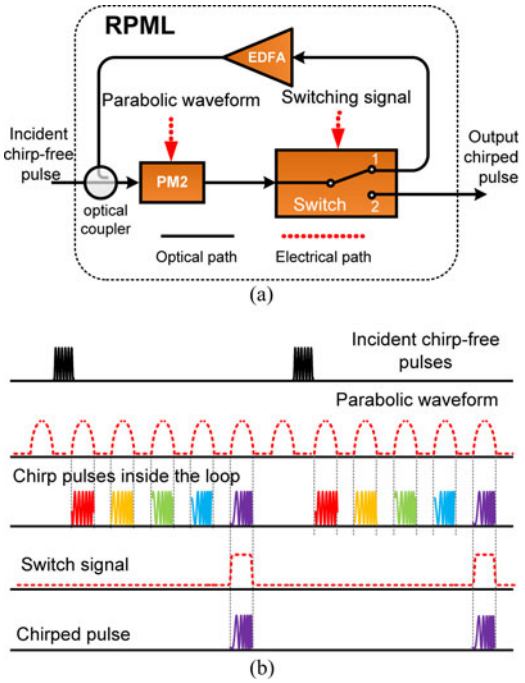

Fig. 2. (a) Schematic of the RPML. (b) Illustration of the multiple-phase-modulation process inside the RPML.

The multiple phase-modulation process inside the RPML is summarized as: 1) when the voltage of the switching signal applied to the switch is zero, the switch is at the "1" state and the incident optical pulse is kept to circulate inside the loop. After amplified by the EDFA to compensate for the loss of the RPML, the pulse is routed back to PM2 via the optical coupler for additional phase modulation. Therefore, the incident pulse will circulate inside the loop, experiencing multiple phase modulations; 2) when the voltage of the switching signal is high, the switch is at the "2" state and the phase-modulated optical pulse will leave the RPML. Therefore, by controlling the time delay between the switching signal applied to the switch and the incident pulse, the incident chirp-free optical pulse is capable of circulating inside the fiber loop for multiple phase modulations. Therefore, the chirp rate of the incident optical pulse is accordingly multiplied, which would lead to a significantly increased bandwidth, leading to an increased TBWP of the generated LCMW. The multiple phase-modulation process of the RPML is illustrated in Fig. 2(b).

C. Linearly Chirped Microwave Pulse Generation

The schematic of the proposed LCMW generation system is shown in Fig. 3. A CW light wave from the TLS is split into two parts by a 1×2 coupler: one is sent to the OEO to generate microwave signal with the lower sideband obtained at the other end of the PS-FBG which is sent to the PD (PD2); the other is sent to the IM to generate a chirp-free optical pulse which is then sent to the RPML to generate a chirped optical pulse with multiplied chirp rate. The chirped optical pulse is then combined with the lower sideband from the OEO at a second coupler, and beat at PD2 to generate an LCMW.

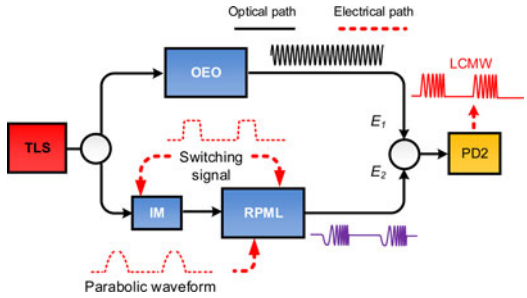

Fig. 3. Schematic of the proposed LCMW generation system.

Mathematically, the two light waves sent to the PD can be expressed as

$$\begin{bmatrix} E_1(t) \\ E_2(t) \end{bmatrix} = \begin{bmatrix} E_{01} \cdot \exp\left[j(2\pi(f_o - f_{\text{osc}})t)\right] \\ E_{02} \cdot s(t) \exp\left[j\left(2\pi f_o t + N\dfrac{\pi V}{V_\pi} c(t)\right)\right] \end{bmatrix} \tag{1}$$

where E_1 and E_2 are the electrical fields of the lower sideband from the OEO and the chirped optical pulse, E_{01} and E_{02} are the amplitudes of E_1 and E_2, respectively, f_o is the frequency of the incident light wave, f_{osc} is the oscillation frequency of the OEO, N is the number of the recirculation times of the optical pulse inside the RPML, $c(t)$ is the normalized parabolic waveform with a temporal duration of $2T_0$, V is its peak-to-peak voltage, V_π is the half-wave voltage of PM2. The parabolic waveform is expressed as

$$c(t) = \begin{cases} Kt^2 + 1, & |t| \le T_0 \\ 0, & \text{else} \end{cases} \tag{2}$$

where K is a constant which is equal to $-1/T_0^2$. The switching signal $s(t)$ can be expressed as

$$s(t) = \begin{cases} 1, & |t| \le T_0 \\ 0, & \text{else.} \end{cases} \tag{3}$$

By beating the two light waves at PD2, an LCMW is generated at the output of PD2, which is given by

$$\begin{aligned} i(t) &\propto ac\left|E_1(t) + E_2(t)\right|^2 \\ &= \begin{cases} \cos\left[2\pi f_{\text{osc}} t + \dfrac{N\pi V}{V_\pi}\left(-\dfrac{t^2}{T_0^2} + 1\right)\right], & |t| \le T_0 \\ 0, & \text{else} \end{cases} \end{aligned} \tag{4}$$

where ac indicates the operation of taking the ac terms of the signal. It can be seen from (4) that a microwave signal with a carrier frequency of f_{osc}, which is linearly frequency-modulated by the parabolic waveform $c(t)$ is generated. The pulse duration of the LCMW is determined by the switching signal $s(t)$. Thus, the temporal duration of the LCMW can be controlled by the switching signal. The carrier frequency f_{osc}, which is the oscillation frequency of the OEO, can be simply tuned by changing the wavelength of the TLS, which ensures excellent frequency agility. The maximum and the minimum instantaneous

frequencies of the LCMW are

$$f_{ins\_\max} = f_{\text{osc}} + NV/(2V_\pi T_0)$$
$$f_{ins\_\min} = f_{\text{osc}} - NV/(2V_\pi T_0) \quad (5)$$

and the TBWP and the chirp rate can be calculated by

$$\text{TBWP} = 2T_0 \left| f_{ins\_\max} - f_{ins\_\min} \right| = \frac{2NV}{V_\pi} \quad (6)$$

$$\text{Chirp Rate} = \left| f_{ins\_\max} - f_{ins\_\min} \right| / 2T_0 = \frac{NV}{2\left(T_0\right)^2 V_\pi}. \quad (7)$$

It can be seen from (6) and (7) that the TBWP and the chirp rate are functions of the recirculating times N. Thus, by controlling the times of recirculation, the TBWP and the chirp rate are significantly increased. For example, if an optical pulse is circulating 50 times in the RPML, V is equal to 10 V, and V_π is 1 V, an LCMW with a TBWP of 1000 can be generated. In addition, from (3) and (4), we can see that the pulse duration and the repetition rate of the LCMWs can be controlled by the switching signal.

Note that the system has two channels, the upper and the lower channels, as shown in Fig. 3. The IM and the PM are incorporated in the lower channel, due to the losses of the IM and the PM, the total optical power loss in the lower channel is larger than that in the upper channel. To balance the optical powers at the outputs of the two channels, power amplification in the lower channel or attenuation in the upper channel should be applied.

III. Experiment

A. Operation of the OEO

We first demonstrate the operation of the OEO and the use of the OEO to generate a lower sideband. As shown in Fig. 1, a CW light wave at around 1549.4 nm from the TLS (Anritsu, MG9638 A) is sent to PM1. A phase-modulated signal is obtained at the output of PM1. The phase-modulated signal consists of an optical carrier, an upper sideband and a lower sideband, which is sent to the PS-FBG, with the lower sideband rejected by the PS-FBG. The optical carrier and the upper sideband are reflected by the PS-FBG and beat at PD1. The beating signal is amplified by the PA and sent back to PM1 to close the OEO loop. Note that the rejected lower sideband is in fact transmitted from the PS-FBG, which is used for LCMW generation. Details about the operation of the tunable OEO and the fabrication of the PS-FBG employed in the OEO can be found in [19] and [20]. Fig. 4 shows the optical spectra of the optical carrier from the TLS and the lower sideband from the OEO by combining the two using an optical coupler and monitored by an optical spectrum analyzer (OSA, Ando AQ6317B). As can be seen, the wavelength spacing between the optical carrier and the lower sideband can be controlled by changing the wavelength of the TLS. From Fig. 4 we can also see that the wavelength of the lower sideband is not changed and the wavelength of the light wave from the TLS is tunable. The smaller peaks located at the left of the optical carrier in Fig. 4 are the upper sideband that is not completely suppressed.

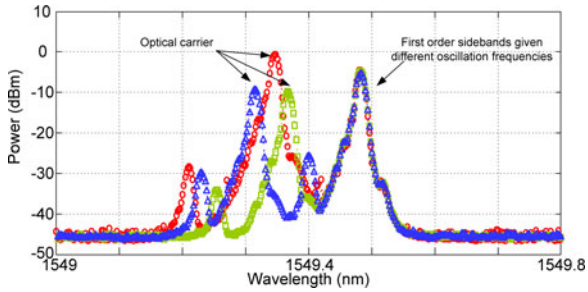

Fig. 4. Measured optical spectra of the light wave from the TLS and the lower sideband from the OEO.

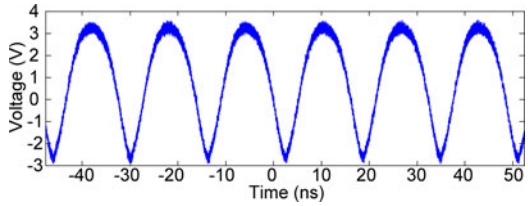

Fig. 5. Measured parabolic waveform used in the experiment.

B. Recirculating-Phase-Modulation Loop

We then demonstrate the generation of a chirped optical pulse with multiplied chirp rate using the RPML. As shown in Fig. 3, part of the light wave from the TLS is sent to an IM to generate a chirp-free optical pulse. The IM is driven by a switching signal from a low-frequency electrical pulse generator (Agilent 33250 A). The generated electrical pulse has a temporal duration of about 15 ns. Thus, the CW light wave is changed to an optical pulse with a temporal duration of about 15 ns.

To demonstrate the operation of the RPML, a parabolic waveform generated by an AWG (Tektronix, AWG7102), shown in Fig. 5, is applied to PM2 in the RPML. To simplify the experiment, the RPML is always kept closed by replacing the optical switch with an optical coupler, thus no synchronization is needed.

Since the optical switch is replaced by an optical coupler, after each circulation, part of the phase-modulated optical pulse is routed out through the optical coupler, thus an optical pulse train is generated for one incident optical pulse applied to the input. In the experiment, to avoid the overlapping between two pulse trains corresponding to two different incident optical pulses, the temporal separation between the two incident optical pulses must be much greater than the fundamental time delay of the RPML, which is about 0.2 μs (corresponding a fundamental resonant frequency of 5 MHz), to ensure that the pulse train resulted from the first incident pulse is completely routed out before the second pulse is injected into the loop. Thus, in the experiment the temporal separation between two incident optical pulse is selected to be 100 μs (corresponding a pulse repetition rate of 10 KHz).

Fig. 6 shows the pulse train after optical to electrical conversion at PD2 (Newport, 25 GHz) and measured by a real time oscilloscope (Agilent, DSO-X93204 A, 80 GSa/s). As can be

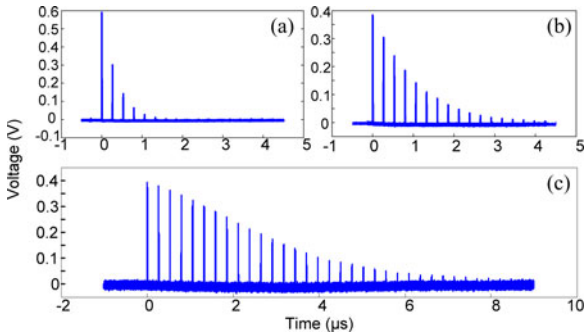

Fig. 6. Measured pulse train at the output of the RPML as the loop loss is decreased by increasing the gain of the EDFA. From (a) to (b) to (c), the loss of the loop is decreasing.

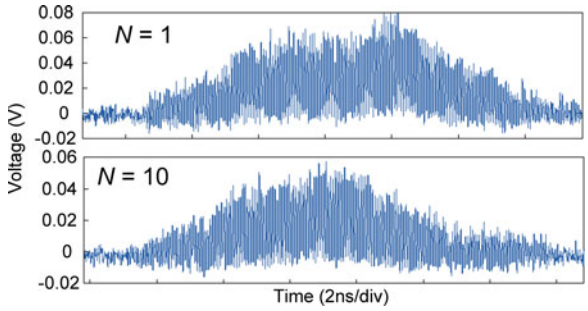

Fig. 7. Measured LCMWs. (a) The LCMW corresponding to the optical pulse circulating in the loop once and (b) the LCMW corresponding to the optical pulse circulating in the loop ten times.

seen as the net loop loss is reduced by increasing the gain of the EDFA, the times of the circulation for one incident optical pulse is increased and more pulses at the output of the RPML can be observed.

In the experiment, the peak-to-peak voltage of the parabolic waveform is about 6 V, the half-wave voltage V_π of PM2 is about 6.5 V, the pulse duration is about 15 ns, after each circulation, based on (6), the bandwidth of the chirped optical pulse is increased by about 120 MHz.

In the optical pulse train, different pulse has different times of phase modulation. The Nth pulse in the train experiences N times phase modulation introduced by the parabolic waveform. As N is increasing, the chirp rate and the bandwidth of the optical pulse are also increasing. Therefore, by heterodyning the optical pulse with a CW light wave, an LCMW with an increased TBWP is generated.

Assume that synchronization is applied and the optical switch is not replaced by an optical coupler, by properly setting the switching signal applied to the optical switch, at the output of the RPML only one optical pulse would be generated, which would experience N times phase modulation, the number of N is determined by the time delay between the switching signal and the incident optical pulse.

C. LCMW Generation

Then, the generation of LCMWs is demonstrated. Again, since the optical switch is replaced by an optical coupler, at the output of the RPML, an optical train with each of the pulse in the pulse train with different chirp rate is obtained. By combining one linearly chirped optical pulse from the pulse train with the lower sideband from the tunable OEO and beat them at PD2 (u^2t, 50 GHz, XPDV2120RA), an LCMW is generated. In the experiment, the OEO is first configured to generate an LCMW with a central frequency at 15 GHz. To do so, the wavelength of the TLS is tuned at about 1549.35 nm. Considering the wavelength of the notch of the PS-FBG is 1549.47 nm, the wavelength difference is 0.12 nm, corresponding to a frequency of 15 GHz. Two LCMWs corresponding to the optical pulse recirculating in the RPML for 1 and 10 times are shown in Fig. 7. The cycles of the LCMWs are densely-spaced which makes it difficult to directly observe the frequency chirping from the waveforms.

To verify that the LCMWs are frequency chirped, we calculate the auto-correlations of the LCMWs to see the pulse compression capability, which are then compared with the auto-correlations of two LCMWs generated by simulations with the same temporal duration of 15 ns and chirp rates, with the results shown in Fig. 8(a) and (b). In the simulations, the LCMWs are produced with an amplitude profile of a raised-cosine function which is close to the amplitude profile of the generated LCMWs. It is known that the use of a raised-cosine amplitude profile will decrease the sidelobes significantly. The bandwidth of the first LCMW is 120 MHz, corresponding to an optical pulse after once circulation, and the bandwidth of the last LCMW is 1920 MHz corresponding to an optical pulse after 16 circulations. Accordingly, the chirp rate is increased from 8 MHz/ns to 128 MHz/ns. As expected, as N increases, the pulse compression capability is also enhanced due to the increase in the chirp rate. The bandwidth or the TBWP is increased by 16 times in our experiment, for the LCMW generated with 16 circulations. In Fig. 8, the experimental results show relatively high sidelobes compared with the simulations, which are caused by the noise introduced by the RPML and the profile distortions of the incident optical pulses through intensity modulation.

In the experiment, the circulation times are limited to about 20, due to the fact that part of the pulse is routed out via the optical coupler after each circulation. The TBWP obtained in the experiment is only 28.8. The TBWP could be significantly improved by optimizing the system and applying synchronization. For example, by using a PM with a smaller the half-wave voltage and a parabolic waveform with higher peak-to-peak voltage, the TBWP can be much bigger. Once synchronization between the incident optical pulse and the parabolic waveform is also applied to the RPML, the circulation times could be increased to 50 or higher. Therefore, a TBWP more than 1000 could be achieved.

D. Frequency Agility

Frequency agility is the ability of a microwave waveform generator in a radar system to quickly switch its operating frequency from one to another. Such ability is very important for a radar system to account for atmospheric effects, jamming, mutual

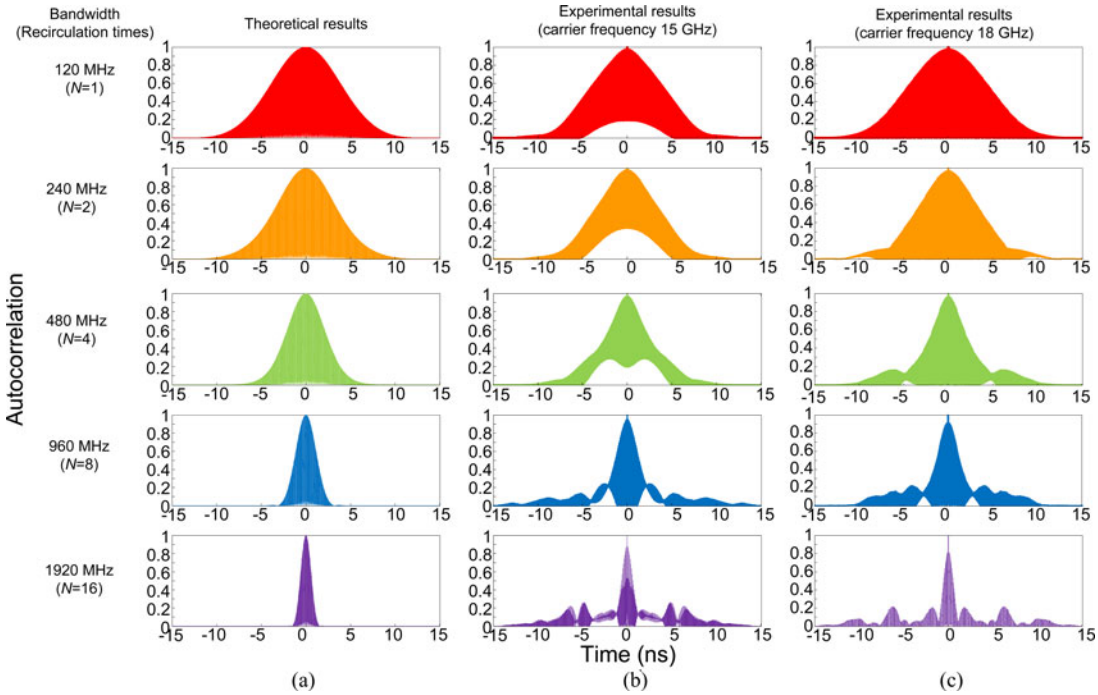

Fig. 8. (a) Simulation results: auto-correlation of 15-ns LCMWs with a bandwidth of 120, 240, 480, 960, and 1920 MHz. (b) Experimental results: auto-correlation of 15-ns LCMWs with a bandwidth of 120, 240, 480, 960, and 1920 MHz corresponding to recirculation of 1, 2, 4, 8, and 16 times. The carrier frequency is 15 GHz. (c) Experimental results: auto-correlation of 15-ns LCMWs with a bandwidth of 120, 240, 480, 960, and 1920 MHz corresponding to recirculation of 1, 2, 4, 8, and 16 times. The carrier frequency is 18 GHz.

interference with friendly sources, or to make it more difficult to locate through radio direction finding. Therefore, to generate an LCMW with a switchable carrier frequency is practically required. In our proposed approach, changing the microwave carrier frequency can be easily and quickly achieved by changing the wavelength of the TLS. To demonstrate the frequency agility, in the experiment the carrier frequency of the LCMW is tuned from 15 to 18 GHz by changing the wavelength of the TLS from 1549.35 to 1549.32 nm. The pulse compression capability of the LCMWs at the new frequency is shown in Fig. 8(c).

The microwave carrier frequency can be further increased [20], and the upper limit is limited by the bandwidth of the PDs, PAs, and PMs as well as the reflection bandwidth of the PS-FBG. Considering the bandwidths of these devices can be as large as 40 GHz, a large frequency tunable range up to 40 GHz can be achieved. The switching speed of the carrier frequency is mainly limited by the loop length of the OEO. Given an OEO with a loop length of hundreds of meters, a switching speed in the order of microseconds can be expected.

IV. Conclusion

A novel approach to generating LCMWs with an increased TBWP based on a tunable OEO and a RPML was proposed and experimentally demonstrated. The key significance of the proposed approach is that the chirp rate of the generated LCMW is significantly increased, leading to a significantly increased TBWP. In addition, the approach allows the generation of a frequency-tunable LCMW without using a separate microwave source.

An experiment was performed. The generation of LCMWs with increased chirp rate corresponding to an increased times of recirculation was demonstrated. In the experiment, the LCMWs after 1, 2, 4, 8, and 16 times of recirculation corresponding to the bandwidths of 120, 240, 480, 960, and 1920 MHz, were generated. The TBWP was increased by 16 times. Due to the fast frequency tuning, the proposed generator exhibited excellent frequency agility. The generated LCMWs also exhibited a good pulse compression performance.

References

[1] D. K. Barton, *Radar System Analysis and Modeling*. Boston, MA, USA: Artech House, 2005.
[2] H. D. Griffiths and W. J. Bradford, "Digital generation of high time bandwidth product linear FM waveforms for radar altimeters," *IEE Proc. Radar and Signal Processing*, vol. 139, no. 2, pp. 160–169, Apr. 1992.
[3] H. Kwon and B. Kang, "Linear frequency modulation of voltage-controlled oscillator using delay-line feedback," *IEEE Microw. Wireless Compon. Lett.*, vol. 15, no. 6, pp. 431–433, Jun. 2005.
[4] L. Gao, X. Chen, and J. P. Yao, "Photonic generation of a phase-coded microwave waveform with ultra-wide frequency tunable range," *IEEE Photon. Technol. Lett.*, vol. 25, no. 10, pp. 899–902, May 2013.
[5] Z. Li, W. Li, H. Chi, X. Zhang, and J. P. Yao, "Photonic generation of phase-coded microwave signal with large frequency tunability," *IEEE Photon. Technol. Lett.*, vol. 23, no. 11, pp. 712–714, Jun. 2011.
[6] Z. Li, M. Li, H. Chi, X. Zhang, and J. P. Yao, "Photonic generation of phase-coded millimeter-wave signal with large frequency tunability using a polarization-maintaining fiber Bragg grating," *IEEE Microw. Wireless Compon. Lett.*, vol. 21, no. 12, pp. 694–696, Dec. 2011.

[7] Y. Zhang and S. Pan, "Generation of phase-coded microwave signals using a polarization-modulator-based photonic microwave phase shifter," *Opt. Lett.*, vol. 38, no. 5, pp. 766–768, Mar. 2013.
[8] L. Wang, W. Li, H. Wang, J. Zheng, J. Liu, and N. Zhu, "Photonic generation of phase coded microwave pulses using cascaded polarization modulators," *IEEE Photon. Technol. Lett.*, vol. 25, no. 7, pp. 678–681, Apr. 2013.
[9] F. Laghezza, F. Scotti, P. Ghelfi, F. Berizzi, and A. Bogoni, "Photonic generation of microwave phase coded radar signal," in *Proc. IET Int. Conf. Radar Syst.*, Oct. 2012, pp. 1–4.
[10] P. Ghelfi, F. Scotti, F. Laghezza, and A. Bogoni, "Photonic generation of phase-modulated RF signals for pulse compression techniques in coherent radars," *J. Lightwave Technol.*, vol. 30, no. 11, pp. 1638–1644, Jun. 2012.
[11] J. D. McKinney, D. E. Leaird, and A. M. Weiner, "Millimeter-wave arbitrary waveform generation with a direct space-to-time pulse shaper," *Opt. Lett.*, vol. 27, no. 5, pp. 1345–1347, Aug. 2002.
[12] C. Wang and J. P. Yao, "Phase-coded millimeter-wave waveform generation using a spatially discrete chirped fiber Bragg grating," *IEEE Photon. Technol. Lett.*, vol. 24, no. 17, pp. 1493–1495, Sep. 2012.
[13] C. Wang and J. P. Yao, "Fourier transform ultrashort optical pulse shaping using a single chirped fiber Bragg grating," *IEEE Photon. Technol. Lett.*, vol. 21, no. 19, pp. 1375–1377, Oct. 2009.
[14] M. Khan, H. Shen, Y. Xuan, L. Zhao, S. Xiao, D. E. Leaird, A. M. Weiner, and M. Qi, "Ultrabroad-bandwidth arbitrary radiofrequency waveform generation with a silicon photonic chip-based spectral shaper," *Nature Photon*, vol. 4, pp. 117–122, Feb. 2010.
[15] A. Zeitouny, S. Stepanov, O. Levinson, and M. Horowitz, "Optical generation of linearly chirped microwave pulses using fiber Bragg gratings," *IEEE Photon. Technol. Lett.*, vol. 17, no. 3, pp. 660–662, Mar. 2005.
[16] H. Gao, C. Lei, M. Chen, F. Xing, H. Chen, and S. Xie, "A simple photonic generation of linearly chirped microwave pulse with large time-bandwidth product and high compression ratio," *Opt. Exp.*, vol. 21, no. 20, pp. 23107–23115, Oct. 2013.
[17] R. Ashrafi, Y. Park, and J. Azana, "Fiber system for DC-free microwave pulse generation with full frequency and chirp reconfigurability," in *Proc. IEEE Top. Meet. Microw. Photon.*, Oct. 2010, pp. 241–244.
[18] W. Li, F. Kong, and J. P. Yao, "Arbitrary microwave waveform generation based on a tunable optoelectronic oscillator," *J. Lightwave Technol.*, vol. 31, no. 23, pp. 3780–3786, Dec. 2013.
[19] W. Li, M. Li, and J. P. Yao, "A narrow-passband and frequency-tunable microwave photonic filter based on phase-modulation to intensity-modulation conversion using a phase-shifted fiber Bragg grating," *IEEE Trans. Microw. Theory Tech.*, vol. 60, no. 5, pp. 1287–1296, May 2012.
[20] W. Li and J. P. Yao, "A wideband frequency-tunable optoelectronic oscillator incorporating a tunable microwave-photonic filter based on phase-modulation to intensity-modulation conversion using a phase-shifted fiber Bragg grating," *IEEE Trans. Microw. Theory Tech.*, vol. 60, no. 6, pp. 1735–1742, Jun. 2012.

Wangzhe Li (S'08) received the B.E. degree in electronic science and technology from Xi'an Jiaotong University, Xi'an, China, in 2004, the M.Sc. degree in optoelectronics and electronic science from Tsinghua University, Beijing, China, in 2007, and the Ph.D. degree in electrical engineering from the University of Ottawa, Canada, in 2013. He is currently a Postdoctoral Researcher working at the Microwave Photonics Research Laboratory, School of Electrical Engineering and Computer Science, University of Ottawa, Ottawa, ON, Canada.

His current research interests include photonic generation of microwave and terahertz signals, arbitrary waveform generation, optoelectronic oscillation, and silicon photonics.

Dr. Li received the 2011 IEEE Microwave Theory and Techniques Society Graduate Fellowship and 2011 IEEE Photonics Society Graduate Fellowship.

Jianping Yao (M'99–SM'01–F'12) received the Ph.D. degree in electrical engineering from the Université de Toulon, France, in December 1997. He joined the School of Electrical Engineering and Computer Science, University of Ottawa, Ottawa, ON, Canada, as an Assistant Professor in 2001, where he became an Associate Professor in 2003, a Full Professor in 2006. He was appointed University Research Chair in Microwave Photonics in 2007. From July 2007 to June 2010, he was the Director of the Ottawa-Carleton Institute for Electrical and Computer Engineering. Prior to joining the University of Ottawa, he was an Assistant Professor in the School of Electrical and Electronic Engineering, Nanyang Technological University, Singapore, from 1999 to 2011.

Dr. Yao has published more than 430 papers, including more than 250 papers in peer-reviewed journals and 180 papers in conference proceedings. He is the Chair of numerous international conferences, symposia, and workshops, including the Vice-TPC Chair of the 2007 IEEE Microwave Photonics Conference, the TPC Co-Chair of the 2009, and 2010 Asia-Pacific Microwave Photonics Conferences, the TPC Chair of the high-speed and broadband wireless technologies subcommittee of the 2009–2012 IEEE Radio Wireless Symposia, the TPC Chair of the microwave photonics subcommittee of the 2009 IEEE Photonics Society Annual Meeting, the TPC Chair of the 2010 IEEE Microwave Photonics Conference, and the General Co-Chair of the 2011 IEEE Microwave Photonics Conference. He received the 2005 International Creative Research Award at the University of Ottawa. He was the recipient of the 2007 George S. Glinski Award for Excellence in Research. He was selected to receive an inaugural OSA outstanding reviewer award in 2012. He is an IEEE Distinguished Microwave Lecturer for 2013–2015.

Dr. Yao is a registered Professional Engineer of Ontario. He is a Fellow of the Optical Society of America, and Canadian Academy of Engineering.